JOC The Journal of Organic Chemistry

Article

pubs.acs.org/joc

Investigation of the Reductive Cleavage of BINAP and Application to the Rapid Synthesis of Phospholes

Chris W. D. Gallop, Mariusz Bobin, Petra Hourani, Jessica Dwyer, S. Mark Roe, and Eddy M. E. Viseux*

School of Life Sciences, Department of Chemistry, University of Sussex, Brighton BN1 9QJ, U.K.

Supporting Information

ABSTRACT: A rapid and easy entry into λ^3-phospholes and λ^4-phosphole oxides derived from BINAP is reported herein featuring a variety of C and Si substituents and functional groups, as well the investigative work on the mechanistic pathway. DFT calculations using B3LYP functionals have been carried out to rationalize the mechanism. The observed experimental ^{31}P resonance shifts were compared with the calculated shifts of the proposed intermediates after calibration of the shielding tensors. The calculations included the use of polarizable continuum models to take into account solvent effects and were found to be in excellent agreement, providing further evidence for the proposed mechanism.

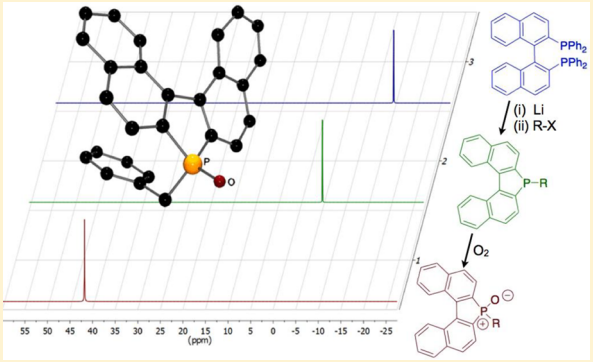

INTRODUCTION

Binaphthyl frameworks and phospholes have widespread applicability which ranges from ligands for transition metals,[1,2] to use as catalysts or as drugs,[3−7] to novel building blocks for materials with unique electronic features that can also be used in self-assembly frameworks,[8−10] to molecular electronics and photonics,[2,11] to π-conjugated polymers.[12] In the context of developing libraries of polydentate ligands based on a binaphthyl framework, we investigated the reductive cleavage of BINAP (**1**) to phospholes. The cleavage of triarylphosphines with lithium metal in THF is a well-known method to generate lithium diarylphosphides ($LiPAr_2$), which are synthetically useful and can be used for further functionalization.[13,14] Other diphosphine ligands have also been lithiated such as dppm and dppe,[15,16] and examples of functionalization of the 2′-position of BINAP to 2-diphenylphosphino-1,1′-binaphthyls[8,17] requires a multistep process as well as the use of BuLi to chemoselectively cleave the P−C bonds of a phosphine oxide in the presence of a phosphine. We report herein on the clean and quantitative reductive cleavage of BINAP to its corresponding lithium phospholide and the one-pot functionalization of the resulting lithium phospholide to silylated and alkylated phospholes and phosphole oxides.

RESULTS AND DISCUSSION

Lithiation Studies. *Experimental Studies.* Preliminary investigation of the stability of a tetraanion of BINAP in the singlet state (HF/6-31G/Opt+Freq) suggested the fragmentation pattern described in Scheme 1 to organolithiums **2**−**4** with no reduction of the aromatic systems to the corresponding cycloalkenes. This postulated lack of any Birch reduction products from BINAP was confirmed by our experiments, though the obtained compound was found to be the binaphthyl phospholide **5**. Literature precedent established that the reduction of BINAP and other arylphosphines was dependent on the choice of solvent,[18] whereby the formation of an electride, as is the case with ammonia, could lead to mixtures of Birch reduced products.[13] The complexation of aromatic phosphine as phosphine−boranes also leads to Birch reduced product.[16]

Scheme 1. Predicted Fragmentation of 1 upon Reductive Cleavage[a]

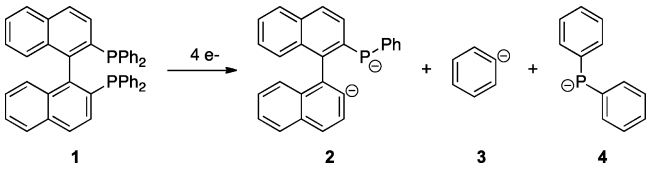

[a]Optimization and frequency calculation at the HF/6-31G+(d) level of theory.

Unlike the reductive cleavage of triphenylphosphine, the reaction of phosphine **1** with lithium proved particularly sensitive to traces of moisture and oxygen, and all reactions had to be performed in a glovebox. The lithiation reactions are typically complete within 48 h. All of the reactions were followed by $^{31}P\{^1H\}$ NMR spectroscopy of the reaction mixtures using Young's NMR tubes equipped with a sealed capillary tube containing $OPPh_3$ in d_6-benzene as an internal standard (δ_P 25 ppm).

Reaction of **1** with lithium metal in THF furnished a dark red solution that exhibited two signals in the $^{31}P\{^1H\}$ NMR spectrum at +50 and −22 ppm. The resonance peak at −22

Received: April 8, 2013
Published: June 4, 2013

   dx.doi.org/10.1021/jo4006393 | J. Org. Chem. 2013, 78, 6522−6528

ppm was identified as $LiPPh_2$ (**4**) by performing the lithiation of PPh_3 and recording the NMR of the mixture of the resulting solutions. Lithium phosphides (such as **4**) typically have negative chemical shifts. This was found to be inconsistent with one of the two $^{31}P\{^1H\}$ signals recorded at 50 ppm. DFT calculations described herein provided a calculated chemical shift of 49 ppm for phospholide **5**. Mathey also reported $^{31}P\{^1H\}$ NMR data for phenyl-substituted phospholides with $^{31}P\{^1H\}$ chemical shifts between +58 and +100 ppm.[19] This strongly suggested that our signal at 50 ppm was a cyclic phospholide (Fgure 1). The

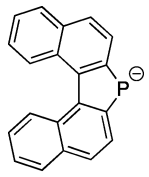

5

Figure 1. Dinaphthylphospholide anion.

structure was subsequently confirmed by negative ESI mass spectroscopy with an accurate mass corresponding to that of **5** and by trapping experiments described herein and X-ray crystallography of the resulting compounds.

The influence of the number of equivalents of lithium on the reaction was also investigated (Table 1). A substoichiometric

Table 1. ^{31}P NMR Data for the Lithiation of Triarylphosphines in THF[a]

entry	compd	amt of lithium (equiv)	$^{31}P\{^1H\}$ δ (ppm)[b]
1	BINAP	0	−14.89 (s)
2	BINAP	4	50.25 (s), −21.67 (s)
3	PPh_3	2	−21.61 (s)
4	BINAP + PPh_3	4 (BINAP), 2 (PPh_3)	50.33 (s), −21.76 (s)

[a]The lithiations were carried out using the general procedure described in the Experimental Section. Reactions were typically complete in 48 h. [b]Multiplicities indicated in parentheses.

amount (2 equiv) led to the partial lithiation of BINAP, and an excess (6 equiv) did not seem to impact negatively on the reaction; products resulting from Birch reduction were never observed in the course of this study, as corroborated by Meijboom in his investigation on other triarylphosphines.[20]

The lithiated solution was reasonably stable over an extended period of time (two months at room temperature under argon), with the appearance of trace signals at −14.9 and −15.9 ppm. The signal at −15.9 ppm was attributed to a small amount of dimerization of **4** to $Ph_2P{-}PPh_2$.[15,21]

DFT Calculations. Shielding tensors were calculated using DFT calculations and then were converted to $^{31}P\{^1H\}$ chemical shifts, in order to support our assignments of the experimentally observed shifts (Table 2). Gas-phase geometry optimizations were performed using Gaussian 09 using the B3LYP/6-31G(d) level of theory; all geometries were confirmed as minima by the absence of imaginary frequencies. The NMR single-point calculations were performed using GIAO-MPW1K/6-311G++(2d,2p) both in the gas phase and using a CPCM (conductor like polarizable continuum) solvent model to obtain the ^{31}P shielding tensors. The MPW1K functional has been shown to be an adequate functional for the calculation of ^{31}P chemical shifts.[22] The authors showed that for GIAO NMR calculations, with an integral equation formalism polarizable continuum solvent

Table 2. Calculated ^{31}P Isotropic Shielding Tensors[a]

entry	compd	σ_{calcd} (CPCM)	σ_{calcd} (IEFPCM)	σ_{calcd} (gas phase)	δ_{exptl} (ppm)
1	$LiPPh_2$	341.83	334.23	302.01	−21.6
2	$HPPh_2$	367.55	367.39	365.42	−40.5
3	$OPPh_3$	299.39	301.07	302.64	24.7
4	PPh_3	327.20	327.25	310.75	−5.0
5	BINAP	334.31	334.34	334.21	−14.9

[a]GIAO-MPW1K/6-311G++(2d,2p)//B3LYP/6-31G(d).

model (IEFPCM), performed both with and without explicit solvent molecules in the geometry optimization gave good results. The solvent was modeled by using polarizable continuum models (IEF and CPCM) to keep the calculations computationally cheap with a level of accuracy sufficient for the rapid determination of $^{31}P\{^1H\}$ shifts of unknown intermediates.

The direct results from GIAO NMR calculations are isotropic shielding tensors (σ); these values must be converted to chemical shift values (δ) using eq 1.

$$\delta_{calcd} = \sigma_{ref} - \sigma_{calcd} \quad (1)$$

In order to determine σ_{ref}, we extended the multistandard approach used for ^1H and ^{13}C by Tantillo, Rablen, and Bally to the ^{31}P nucleus.[23,24] The linear regression for calculated ^{31}P isotropic shielding tensors against experimental ^{31}P shifts was performed using five known compounds (PPh_3, PPh_3O, BINAP, $LiPPh_2$, and $HPPh_2$). As expected, the plot of the gas-phase calculated shielding tensors against experimental chemical shifts gave a poor correlation with a low R^2 value (0.55) (Figure 2). The

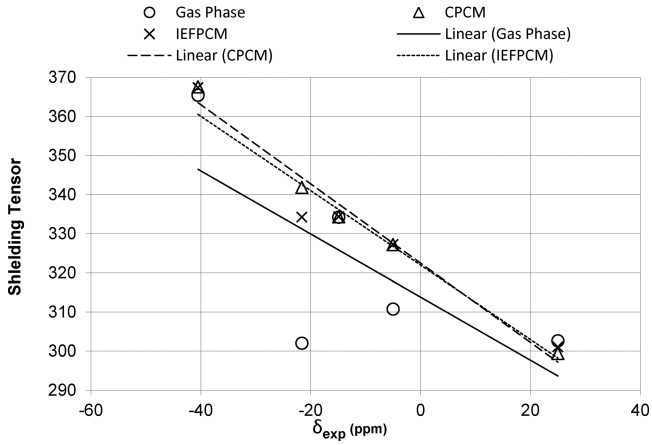

Figure 2. Linear regression of the calculated shielding tensors vs experimental chemical shifts. Regression and R^2 values: (i) gas phase, $y = -0.8069x + 313.81$, $R^2 = 0.51743$; (ii) IEFPCM, $y = -0.9519x + 322.01$, $R^2 = 0.94281$; (iii) CPCM, $y = -1.0136x + 322.5$, $R^2 = 0.98416$.

solvent is known to have an impact on both the calculated and the experimental shifts. This was further demonstrated by the linear regression of ^{31}P isotropic shielding tensors against experimental ^{31}P shifts obtained using IEFPCM solvation ($R^2 = 0.94$) and a CPCM ($R^2 = 0.98$). CPCM solvation was chosen for the purpose of this study. The intercept of the regression line with the y axis provided the shielding tensor value for 0 ppm, which was used as a reference for calculated chemical shifts as shown in eq 1.

dx.doi.org/10.1021/jo4006393 | J. Org. Chem. 2013, 78, 6522−6528

The ^{31}P NMR shifts for the postulated species and intermediates of the lithiation reaction (Figure 3) were calculated using this methodology, with σ_{ref} determined as 322.5.

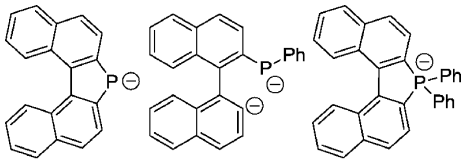

Figure 3. Postulated species involved in the lithiation of BINAP.

The unusual shift observed at 50.3 ppm was initially thought to pertain to structure **2** or **6**, but DFT calculations estimated their chemical shifts at −14.8 and −96.9 ppm, respectively. Of note, a shift at −15.0 ppm was observed in trace quantities when the lithiated solution was left over a period of 15 days. Most importantly, the calculated shift of 49.3 ppm for cyclic dinaphthylphospholide **5** is in agreement with the observed shift, validating the involvement of lithium phospholide **5** in the postulated mechanism (Scheme 3). This equation shows good agreement with the experimental chemical shift (±10%), as shown in the Supporting Information.

Protonation Studies. The mechanisms reported for the lithiation of diphosphines often involve complex equilibria.[15,21] Wild found that the presence of a phosphorus-based radical dianion could affect the outcome of the hydrolysis, which could follow various pathways. The burgundy color of the reaction mixture is characteristic of the formation of radical anions,[8] and the addition of water to the dark red solution changes the color to yellow. Comparative experiments were carried out between the hydrolysis of lithiated Ph_3P and lithiated BINAP (Table 3). The

Table 3. ^{31}P NMR and $^{31}P\{^1H\}$ NMR after Hydrolysis[a]

entry	reactants	$^{31}P\{^1H\}$ δ (ppm)	^{31}P δ (ppm)
1	BINAP + 4 Li	−40.59 (s), 48.76 (s, trace)	−40.60 (d, J = 216.2 Hz), 48.76 (s, trace)
2	PPh_3 + 2 Li	−40.52 (s)	−40.51 (d, J = 218.7 Hz)
3	{BINAP + 4 Li} + {PPh_3 + 2 Li}[b]	−40.48 (s)	−40.48 (d, J = 217.7 Hz)

[a]Multiplicity and J values indicated in parentheses. [b]Approximately equal quantities of entry 1 and entry 2 were mixed in an NMR tube.

former experiment showed the disappearance of the singlet at −21.6 ppm and the appearance of a doublet at −40.5 ppm (J = 218.7 Hz) in the proton-coupled ^{31}P NMR spectrum which overlapped with that of the hydrolysis of the lithiated BINAP.

^{t}BuCl is often used to quench organolithium byproducts in phosphine lithiation reactions, and the protolysis with this weaker acid gave a different result. The use of 2 equiv was shown to rapidly protonate PhLi. Upon addition of another 1 equiv of ^{t}BuCl, the protonation of $LiPPh_2$ was found to be much slower (typically 6 h at room temperature), with little to no change in color, the solution retaining a dark burgundy color. $^{31}P\{^1H\}$ NMR spectroscopy showed the disappearance of the signal at −22 ppm and the appearance of a doublet at −40.5 ppm. Interestingly, the phospholide at 50 ppm did not react with a slight excess of ^{t}BuCl, even when left for over 1 month. With a 12-fold excess, however, the phospholide signal disappeared and the peak for $HPPh_2$ (−40.5 ppm) was the only signal observed. Of note, no nucleophilic substitution was observed between the lithium phosphide and phospholide and ^{t}BuCl as previously reported.[25]

Interestingly, the use of a strong acid gave a very different outcome to the previous proton sources. When methanesulfonic acid (5 equiv) was used, two new doublets appeared, corresponding to $HPPh_2$ (−40.5 ppm) and to protonated **5** (−62 ppm, d, J = 198.5 Hz), which was observed by Gladiali using a different route and is consistent with the formation of a P−H bond. [20]

Silylation Studies. We initially attempted to trap the lithiated species as boron adducts, but ^{11}B NMR proved inconclusive. Different trapping experiments were attempted using silanes to form silylated phosphines useful in addition[26] and cross-coupling reactions.[27] We have shown here that the lithiated phosphides and phospholides can be cleanly trapped as their silylated analogues. TMSCl and TMSOTf were both successful in trapping the lithium phosphide species and gave three signals by $^1H/^{29}Si$ HMBC and two singlets by $^{31}P\{^1H\}$ NMR at −58.53 and −58.69 ppm (Table 4).

Table 4. $^{31}P\{^1H\}$ NMR Data for TMS-Derived Reaction Mixtures

entry	compd	amt of TMSOTf (equiv)	$^{31}P\{^1H\}$ δ (ppm)[a]
1	BINAP + 4 Li	4	−58.53 (s), −58.69 (s)
2	PPh_3 + 2 Li	2	−58.60 (s)
3	{BINAP + 4 Li} + {PPh_3 + 2 Li}[b]	4 (BINAP), 2 (PPh_3)	−58.54 (s), −58.69 (s)

[a]Multiplicity indicated in parentheses. [b]Approximately equal quantities of entry 1 and entry 2 were mixed in an NMR tube.

The lithiated reaction mixtures were also trapped with the more sterically hindered TBSOTf. The singlets were obtained at −61.9 ppm ($TBSPPh_2$) and at −57 ppm (P-silylated dinaphthylphosphole) (Table 5). A small amount of the hydrolyzed diphenylphosphide was also observed at −40.5 ppm, likely due to a trace amount of trifluoromethanesulfonic acid.

Table 5. $^{31}P\{^1H\}$ NMR Data for TBS-Derived Reaction Mixtures

entry	compd	amt of TBSOTf (equiv)	$^{31}P\{^1H\}$ δ (ppm)[a]
1	BINAP + 4 Li	4	−40.45 (s) trace, −57.06 (s), −61.86 (s)
2	PPh_3 + 2 Li	2	−40.44 (s) trace, −61.87 (s)
3	{BINAP + 4 Li} + {PPh_3 + 2 Li}[b]	4 (BINAP), 2 (PPh_3)	−40.53 (s) trace, −57.15 (s), −61.95 (s)

[a]Multiplicity indicated in parentheses. [b]Approximately equal quantities of entry 1 and entry 2 were mixed in an NMR tube.

The difference in reactivity between lithium phosphide **4** and lithium phospholide **5** was demonstrated by using a less reactive silane, and reaction with TBSCl with dinaphthylphospholide was found to be very slow (typically 12 h). Treatment with water resulted in the facile cleavage of the P−Si bond, as $^{31}P\{^1H\}$ NMR of the crude reaction mixture solely showed signals at −40.5 ppm ($HPPh_2$) and −62 ppm (phosphole-H).

Alkylation Studies. The synthesis of binaphthylphospholides is a multistep process involving arylphosphole intermediates obtained by either nucleophilic substitutions on highly toxic

dx.doi.org/10.1021/jo4006393 | J. Org. Chem. 2013, 78, 6522−6528

aryldichlorophosphines[20] or reduction of bis-phosphine monoxides with a large excess of *n*-butyllithium.[8,28] The access to phospholides subsequently requires an extra reductive step to cleave the C−P bond. The direct lithiation of BINAP allows a convenient one-pot access to structurally diverse dinaphthylphospholes utilizing the intermediary phospholide **5** with a variety of electrophiles (Scheme 2). The reactions were

Scheme 2. Preparation of Alkylated Dinaphthylphosphole Oxides[a]

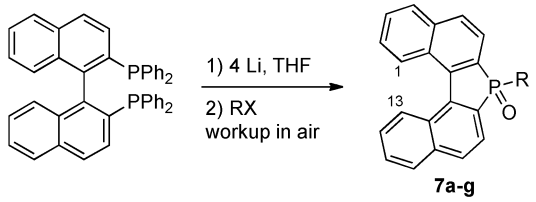

7a-g

Entry	Product	R	Yield (%)[a]
1	**7a**		36
2	**7b**	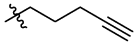	56
3	**7c**		40
4	**7d**		42
5	**7e**		40[b]
6	**7f**	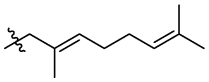	37
7	**7g**	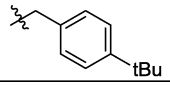	19

[a]Isolated yield after purification and recrystallization. All reactions showed 100% conversion by $^{31}P\{^{1}H\}$ NMR spectroscopy except for the oxidation of entry 5. [b]90% conversion by NMR.

monitored by ^{31}P NMR spectroscopy, and the signals of all alkylated phospholes were observed between −17 and 8 ppm. Of note, a color change also proved useful as an indicator, with changes from dark red for the lithiated species to pale yellow upon treatment with a slight excess of alkyl halide. The rate of color change was dependent on the halide used and the nature of the electrophile. Tertiary halides failed to give any substituted phospholes. The corresponding oxides, with ^{31}P NMR signals ranging from 30 to 50 ppm, were obtained after workup and purification in air. Interestingly and in contrast to all the other analogues, the cyclobutyl phosphole required extended vigorous stirring in air to convert to its corresponding oxide.

$^{13}C\{^{1}H\}$ NMR spectra of the alkylated dinaphthyl phosphole oxides gave indications of the fluxional behavior of the binaphthyl backbone, as previously observed by Gladiali.[20] Broad signals in the aromatic region corresponding to C1 and C13 (Scheme 2) are consistently observed for all our substrates. The broad signals are not due to poorly resolved $^{13}C-^{31}P$ coupling, as no resolution was observed in a $^{13}C\{^{31}P\}$ experiment. This broadening is attributed to the dynamic exchange between the various conformers of the binaphthyl backbone. The α and β aliphatic carbon atoms show a clear coupling with the phosphorus atom, which is absent in the $^{13}C\{^{31}P\}$ experiment (Figure 4A).

The aliphatic region of the ^{1}H NMR shows two distinct multiplets for the β protons at 1.48−1.61 and 1.72−1.84 ppm at −30 °C (Figure 4B). These signals coalesce when the

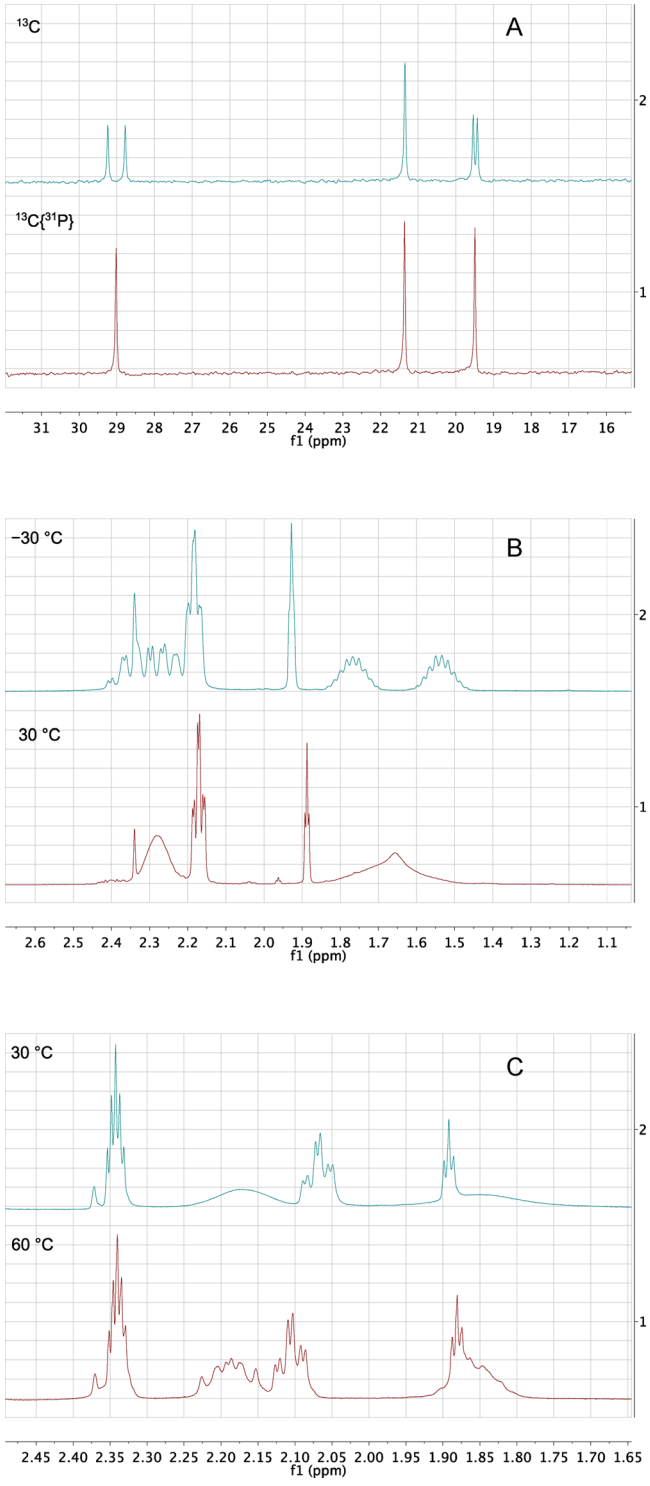

Figure 4. NMR data supporting dynamic exchange of the binaphthyl backbone for oxide **7b**: (A) comparison of ^{13}C and $^{13}C\{^{31}P\}$ spectra in $CDCl_3$ showing the aliphatic region; (B) comparison of ^{1}H NMR spectra in $CDCl_3$ at variable temperatures, with toluene used as internal standard (δ_H 2.34); (C) comparison of ^{1}H NMR spectra in toluene-d_8 at variable temperatures.

temperature is raised, which rules out diastereotopic protons and suggests the existence of two distinct atropoisomers. The signals of the α protons (multiplet between 2.15 and 2.45 ppm) are also resolved at low temperature but overlap for both conformers. The effective line width of the signal due to the

dx.doi.org/10.1021/jo4006393 | J. Org. Chem. 2013, 78, 6522−6528

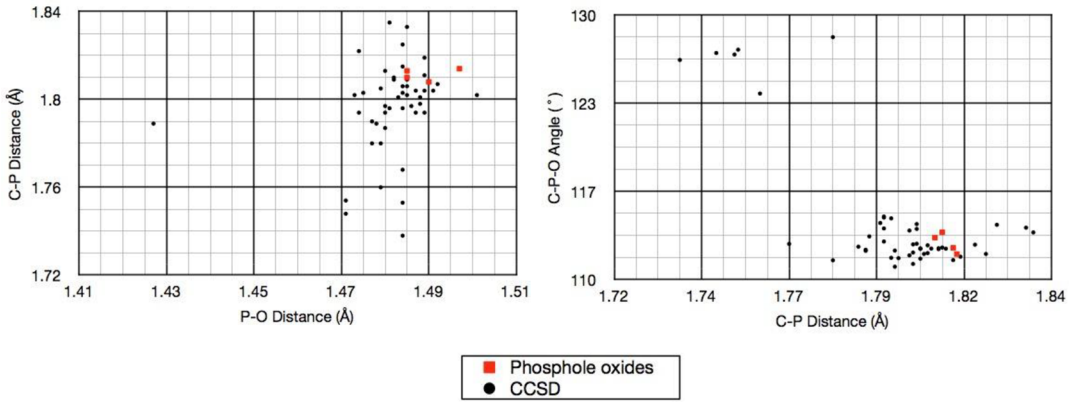

Figure 5. Comparative graphs between C−P distances and C−P−O angles around the P center.

exchange process is greater than the coupling constant at 30 °C, and the broad signals observed for the α and β protons are indicative of an intermediary state of exchange on the NMR time scale. In the fast exchange limit, at higher temperature (Figure 4C), the peaks narrow and the coupling begins to resolve. All observations are consistent with exchange between the atropoisomers of the binaphthyl backbone.

Oxides **7a−e** yielded crystals that were suitable for X-ray diffraction studies. In all cases, full structural data are included in the Supporting Information. The molecular structures of these complexes all contain a tetracoordinate phosphorus atom linked to an oxygen atom with unexceptional P−O and P−C bond distances and C−P−O bond angles. Inspection of the CCSD showed that, of the 39 structures that contain phospholes, all are tetrahedral at the phosphorus atom, with conventional distances except for those where the system is particularly structurally constrained or complexed to a transition metal (Figure 5). All of the obtained structures show that the formation of a five-membered phosphole introduced strain in the naphthyl backbone and caused the fused naphthyl rings to distort and pucker in comparison with BINAP (Figure 6). Gladiali also observed this change in conformation in his studies of diastereomeric equilibration of a *P*-alkyl bis-naphthyl phosphole.[20] The distortion causes a decrease in steric clash between H13 and H8 (Figure 6). This appears to reduce the energy barrier in comparison to BINAP, as the exchange process between the two atropoisomers is observed at 30 °C by NMR.

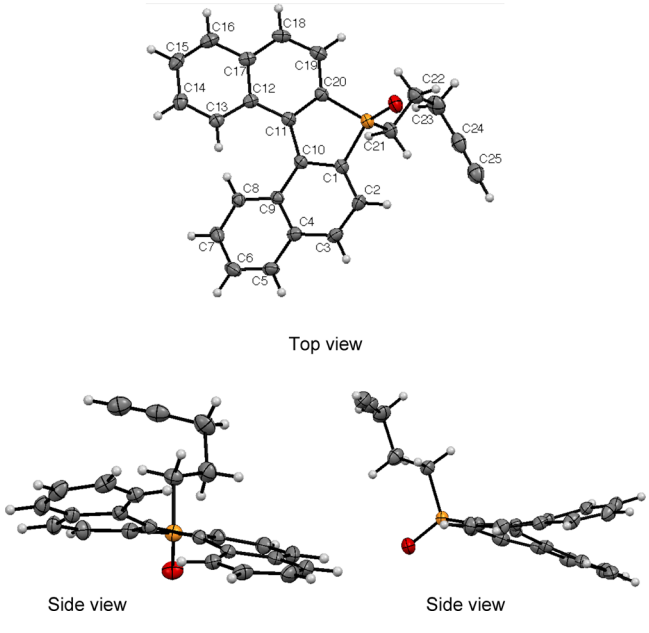

Figure 6. Solid-state structure of **7b**.

Postulated Mechanism. On the basis of the observations presented herein, we propose the mechanism highlighted in Scheme 3. The first 2 equiv of lithium reductively cleaves the phosphorus−$C_{naphtyl}$ bond to yield the corresponding lithiated aromatic species **8** and $LiPPh_2$ (**4**) as a byproduct. The steric hindrance imparted by the diphenylphosphine groups is relieved and allows the binaphthyl C−C bond to rotate. During rotation it can form the reactive and electron-rich P(V) phosphoranide **6**, as previously postulated by Hayashi in 2001[8] and further supported by a potential energy surface (PES) scan in this study (Figure 7). The initial dihedral angle used for intermediate **8** was assumed to be approximately the same as that of BINAP (87°).[29] Interestingly, intermediate **6** (dihedral angle of −32°) was found to have the lowest energy of all possible structures when scanning dihedral angles from −88 to 272° with increments of 1°.

Intermediate **6** can then undergo a facile, rapid, and irreversible elimination of phenyllithium to phosphole **9**. Phosphole **9** was never observed by NMR but is known to react rapidly with lithium to yield the corresponding phospholide **5**.[20] This mechanism may also occur via a radical pathway, as

Scheme 3. Proposed Mechanism for the Reductive Cleavage of 1 with 4 equiv of Li Metal[a]

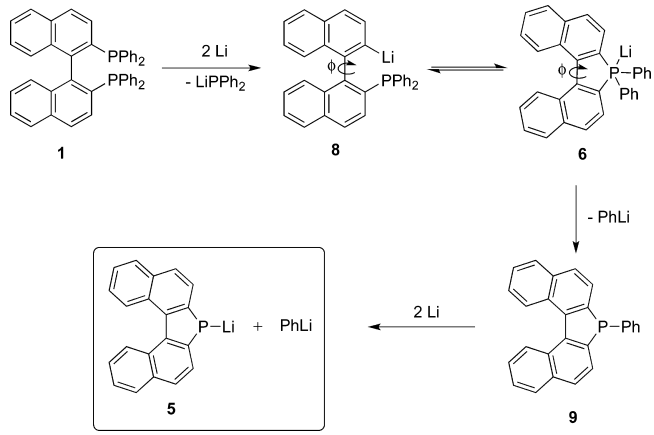

[a]The dihedral angles ϕ of intermediates **8** and **6** are −88 and −32°, respectively.

dx.doi.org/10.1021/jo4006393 | J. Org. Chem. 2013, 78, 6522−6528

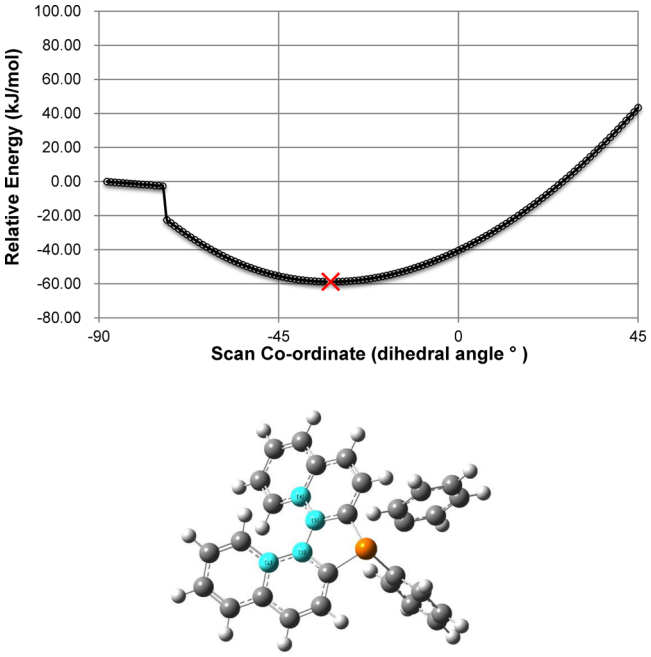

Figure 7. Plot of the PES of intermediate **8** on varying the dihedral angle (defined by highlighted atoms in the structure given below the plot) through 360° with increments of 1°. The relaxed PES scan was carried out at the B3LYP/6-31G(d) level of theory.The lowest energy structure (marked with a cross) is depicted in the plotand corresponds to intermediate **6**. Structures were modeled as anions without explicit Li atoms.

highlighted in previous studies into the reductive cleavage of arylphosphines.[25]

CONCLUSIONS

We have reported herein a thorough investigation of the reductive cleavage of commercially available BINAP to form lithiated dinaphthylphospholide, along with a suggested mechanism. Its reactivity and potential are demonstrated by examples of one-pot substitution to silylated and alkylated dinaphthylphospholes, bearing a variety of functional groups useful for further functionalization. We have also confirmed and extended the usefulness of DFT calculations for predicting ^{31}P chemical shifts as a tool for identifying unknown compounds and intermediates in synthesis.

EXPERIMENTAL SECTION

General Methods. Starting materials and reagents were purchased from commercial sources and were used without any prior purification unless otherwise noted. Both TMS triflate and TBS triflate were purified by distillation under an inert atmosphere. All solvents were dried and distilled using standard methods. ^1H NMR and ^{13}C NMR spectra were collected at 30 °C in $CDCl_3$ using a 500 MHz spectrometer (500 and 125 MHz, respectively), and referenced using the residual solvent signal (δ_H 7.27, δ_C 77). $^{13}C\{^{31}P\}$ NMR spectra were recorded on a 600 MHz spectrometer at 150.81 MHz. The majority of ^{31}P NMR spectra were carried out in THF with a sealed capillary tube containing $OPPh_3$ in d_6-benzene as an internal standard (δ_P 25). ^{31}P NMR of the phosphole oxides was carried out in $CDCl_3$ and referenced to an 85% aqueous solution of H_3PO_4 (δ_P 0). ^{31}P NMR spectra were collected at 30 °C using a 400 MHz spectrometer (161.72 MHz). The IR spectra were recorded using a FT-IR spectrometer equipped with an ATR accessory with a diamond top plate. High-resolution mass spectra were obtained using ESI in either positive or negative mode with a Brucker Daltonics Epics III 4.7 T Fourier transform ion cyclotron resonance mass spectrometer. Unless stated otherwise, all reactions were carried out in a glovebox or on a Schlenk line.

General Procedure for the Lithiation of Phosphines. The lithiations were carried out on a 0.01 M solution of the desired phosphine in a Young's ampule equipped with a glass stirrer bar.[29] The appropriate amount of lithium was weighed and cut into small pieces and cleaned with fine glass paper.[30] Upon addition the reaction mixture changed from colorless to yellow, typically within 30 s of addition. The reaction mixtures were stirred vigorously for 2−7 days, until no lithium metal was visible and the solution was burgundy in color. $^{31}P\{^1H\}$ NMR of the solution routinely showed peaks at 50 and −22 ppm upon completion.

General Procedure for the Trapping of the Lithiated Solutions. The required amount of the lithiated solution was syringed into an ampule or a glass vial and the necessary trapping reagent added. Most quenching agents were handled and added in the glovebox or, alternatively, by standard Schlenk techniques.

General Procedure for the Alkylation of Binaphthylphosphoholes. A solution of lithiated BINAP (0.16 mmol) was syringed into an ampule or a glass vial, and the requisite alkyl halide (0.64 mmol) was added in one portion. The solution was left at room temperature until ^{31}P NMR showed the disappearance of the peaks at 50 and −22 ppm and the appearance of two new peaks between 0 and −15 ppm. The resultant solution was then removed from the glovebox, quenched with saturated ammonium chloride solution, and extracted with dichloromethane. The combined organic layers were washed with water and brine, dried over sodium sulfate, filtered, and evaporated under reduced pressure to yield a yellow oil. The phosphine oxides were separated by flash chromatography[31] using a gradient solvent system (80 to 100% EtOAc in hexanes) to give a yellow waxy solid, which was further purified by recrystallization from toluene and hexanes.

*7-Benzyl-7H-benzo[e]naphtho[2,1-b]phosphindole 7-oxide (**7a**):* synthesized as a pale yellow solid (22.4 mg, 36%); R_f (60/40, EtOAc/hexanes) 0.32; mp 195.7−196.7 °C; ^1H NMR ($CDCl_3$, 500 MHz) δ_H 8.20−7.91 (m, 6H), 7.90−7.66 (m, 1H), 7.61 (t, J = 7.5 Hz, 2H), 7.48 (t, J = 7.7 Hz, 2H), 6.99 (dt, J = 14.7, 7.7 Hz, 3H), 6.91−6.82 (m, 2H), 3.76−3.22 (m, 2H); ^{13}C NMR ($CDCl_3$, 125 MHz) δ_C 137.2 (s), 131.2 (d, J = 7.6 Hz), 129.9 (s, br), 129.6 (d, J = 5.3) 128.6 (s, br), 128.0 (d, J = 3.0 Hz), 127.9 (s, br), 127.45 (s), 126.7 (d, J = 3.4 Hz), 125.61 (s, br), 124.46 (s, br), 38.2 (d, J = 63.9 Hz); $^{31}P\{^1H\}$ NMR ($CDCl_3$, 162 MHz) δ_P 41.8 (s); IR (neat, ν_{max}, cm^{-1}) 3039, 2939, 1497, 1334, 1232, 1205, 1175, 1145, 881, 818, 748, 700, 657; HRMS $C_{27}H_{19}OPNa$ mass calcd 413.1071, mass found 413.1071.

*7-(Pent-4-yn-1-yl)-7H-benzo[e]naphtho[2,1-b]phosphindole 7-oxide (**7b**):* synthesized as a yellow solid (32.7 mg, 56%); R_f (75/25, EtOAc/hexanes) 0.29; ^1H NMR ($CDCl_3$, 500 MHz) δ_H 8.17 (d, J = 8.6 Hz, 2H), 8.05 (dd, J = 8.1, 3.4 Hz, 2H), 7.98 (q, J = 8.2 Hz, 4H), 7.64 (t, J = 7.5 Hz, 2H), 7.53 (dd, J = 8.4, 7.0 Hz, 2H), 2.38−2.24 (m, 2H), 2.20 (td, J = 6.9, 2.5 Hz, 2H), 1.91 (t, J = 2.7 Hz, 1H), 1.68 (s br, 2H); ^{13}C NMR ($CDCl_3$, 125 MHz) δ_C 137.3 (s), 130.3 (s, br), 128.9 (s), 128.8 (s), 128.0 (s), 127.6 (s), 125.8 (s), 123.9 (s, br), 82.6 (s), 69.6 (s), 29.1 (d, J = 69.9 Hz), 21.4 (d, J = 2.1 Hz), 19.5 (d, J = 16.7 Hz); $^{31}P\{^1H\}$ NMR ($CDCl_3$, 162 MHz) δ_P 43.7 (s); IR (neat, ν_{max}, cm^{-1}) 3250, 3043, 2944, 1445, 1338, 1186, 1147, 966, 883, 821, 757, 729, 657; HRMS $C_{25}H_{20}OP$ mass calcd 367.1252, mass found 367.1248.

*7-Isopropyl-7H-benzo[e]naphtho[2,1-b]phosphindole 7-oxide (**7c**):* synthesized as a pale yellow solid (22.0 mg, 40%); R_f (80/20, EtOAc/hexanes) 0.30; ^1H NMR ($CDCl_3$, 500 MHz) δ_H 8.15 (d, J = 8.6 Hz, 2H), 8.07−7.91 (m, 6H), 7.63 (t, J = 8.2, 2H), 7.52 (t, J = 8.4 Hz, 2H), 2.43 (sept, J = 7.3 Hz, 1H), 1.12 (s, 6H); ^{13}C NMR ($CDCl_3$, 125 MHz) δ_C 137.12 (s), 129.9 (s, br), 128.8 (s), 128.7 (s), 128.0 (s), 127.4 (s), 125.7 (s), 124.4 (s, br), 110.0 (s), 29.0 (d, J = 70.5 Hz), 15.69 (s); $^{31}P\{^1H\}$ NMR ($CDCl_3$, 162 MHz) δ_P 51.3 (s); IR (neat, ν_{max}, cm^{-1}) 3050, 2965, 2926, 2869, 1662, 1443, 1338, 1257, 1198, 1178, 1133, 1026, 886, 814, 749, 692, 654; HRMS $C_{23}H_{20}OP$ mass calcd 343.1252, mass found 343.1236.

*7-Allyl-7H-benzo[e]naphtho[2,1-b]phosphindole 7-oxide (**7d**):* synthesized as a yellow solid (23.0 mg, 42%); R_f (80/20, EtOAc/hexanes) 0.26; mp 213.9−214.5 °C; ^1H NMR ($CDCl_3$, 500 MHz) δ_H 8.16 (d, J = 8.6 Hz, 2H), 8.07−7.92 (m, 6H), 7.63 (t, J = 7.1 Hz, 2H),

dx.doi.org/10.1021/jo4006393 | J. Org. Chem. 2013, 78, 6522−6528

7.53 (ddd, J = 8.3, 6.8, 1.3 Hz, 2H), 5.64 (dddt, J = 17.5, 10.1, 7.5, 5.4 Hz, 2H), 5.12−4.93 (m, 2H), 3.01 (s br, 2H); ^{13}C NMR ($CDCl_3$, 125 MHz) δ_C 137.2 (s), 130.1 (s, br), 128.8 (s), 128.7 (s), 128.7 (s), 128.0 (s), 127.5 (s), 126.7 (d, J = 8.9 Hz), 125.7 (s), 124.2 (s, br), 120.6 (d, J = 12 Hz), 35.8 (d, J = 66.3 Hz); ^{31}P{^{1}H} NMR ($CDCl_3$, 162 MHz) δ_P 40.8 (s); IR (neat, ν_{max}, cm^{-1}) 3043, 2936, 1444, 1420, 1334, 1221, 1183, 1146, 1027, 985, 915, 882, 818, 774, 749, 663; HRMS $C_{23}H_{18}OP$ mass calcd 341.1108, mass found 341.1095.

*7-Cyclobutyl-7H-benzo[e]naphtho[2,1-b]phosphindole 7-oxide (**7e**):* synthesized as a yellow solid (22.7 mg, 40%); R_f (80/20, EtOAc/hexanes) 0.26; ^{1}H NMR ($CDCl_3$, 500 MHz) δ_H 8.16 (d, J = 8.6 Hz, 2H), 8.03−7.93 (m, 6H), 7.62 (t, J = 7.2 Hz, 2H), 7.52 (d, J = 7.0 Hz, 2H), 2.96 (td, J = 8.9, 4.2 Hz, 1H), 2.76−2.02 (m, 4H), 1.96 (dt, J = 9.9, 4.4 Hz, 1H); ^{13}C NMR ($CDCl_3$, 125 MHz) δ_C 137.2 (s), 130.0 (s, br), 128.8 (s), 128.7 (s), 128.0 (s), 127.4 (s), 125.6 (s), 124.3 (s, br), 33.64 (d, J = 71.2 Hz), 22.1 (d, J = 5.2 Hz), 20.4 (d, J = 15.7 Hz); ^{31}P{^{1}H} NMR ($CDCl_3$, 162 MHz) δ_P 43.9 (s); IR (neat, ν_{max}, cm^{-1}) 3045, 2979, 2933, 2858, 1572, 1443, 1339, 1182, 1148, 1003, 907 812, 749; HRMS $C_{24}H_{20}OP$ mass calcd 355.1246, mass found 355.1252.

*(E)-7-(3,7-Dimethylocta-2,6-dien-1-yl)-7H-benzo[e]naphtho[2,1-b]phosphindole 7-oxide (**7f**):* synthesized as a pale yellow solid (26.4 mg, 37%); R_f (80/20, EtOAc/hexanes) 0.33; ^{1}H NMR ($CDCl_3$, 500 MHz) δ_H 8.13 (d, J = 8.6 Hz, 2H), 8.06−7.89 (m, 6H), 7.60 (t, J = 7.5 Hz, 2H), 7.50 (t, J = 7.7 Hz, 2H), 5.01−4.76 (m, 2H), 3.00 (d, J = 15.5 Hz, 2H), 1.78−1.59 (m, 4H), 1.57 (s, 3H), 1.40 (s, 3H), 1.27 (d, J = 3.9 Hz, 3H); ^{13}C NMR ($CDCl_3$, 125 MHz) δ_C 141.2 (d, J = 12.5 Hz), 137.1 (s), 131.5 (s), 130.0 (s, br), 128.7 (s), 127.9 (s), 127.4 (s), 125.6 (s), 124.1 (s, br), 123.7 (s), 111.7 (d, J = 8.7 Hz), 39.4 (d, J = 2.9 Hz), 34.1 (s), 30.5 (d, J = 67.2 Hz), 17.5 (s), 16.4 (d, J = 2.8 Hz); ^{31}P{^{1}H} NMR ($CDCl_3$, 162 MHz) δ_P 42.6 (s); IR (neat, ν_{max}, cm^{-1}) 3192. 3050, 2967, 2918, 2850, 1443, 1336, 1178, 1140, 1026, 970, 864, 815, 748, 730; HRMS $C_{30}H_{30}OP$ mass calcd 437.2029, mass found 437.2040.

*7-(4-(tert-Butyl)benzyl)-7H-benzo[e]naphtho[2,1-b]phosphindole 7-oxide (**7g**):* synthesized as a pale yellow solid (13.5 mg, 19%); R_f (80/20, EtOAc/hexanes) 0.24; mp 179.2−183.3 °C; ^{1}H NMR ($CDCl_3$, 500 MHz) δ_H 8.08−7.91 (m, 6H), 7.89−7.71 (m, 1H), 7.60 (dd, J = 8.1, 6.9 Hz, 2H), 7.53−7.39 (m, 2H), 6.95 (d, J = 8.0 Hz, 2H), 6.77 (dd, J = 8.2, 2.4 Hz, 2H), 3.49 (d, J = 67.8 Hz, 2H), 1.12 (s, 9H); ^{13}C NMR ($CDCl_3$, 125 MHz) δ_C 149.6 (s), 137.1 (s), 129.2 (d, J = 5.2 Hz), 128.6 (s, br), 127.8 (d, J = 7.4 Hz), 127.4 (s), 125.6 (s, br), 124.8 (d, J = 3.0 Hz), 124.4 (s, br), 37.6 (d, J = 64.3 Hz), 34.3 (s), 31.2 (s); ^{31}P{^{1}H} NMR ($CDCl_3$, 162 MHz) δ_P 42.5 (s); IR (neat, ν_{max}, cm^{-1}) 3051, 2960, 2906, 2898, 1507, 1455, 1336, 1206, 1142, 1024, 882, 812, 746, 723; HRMS $C_{31}H_{27}NaOP$ mass calcd 469.1692, mass found 469.1712.

Crystallography. All crystallographic details for compounds **7a**−**e** (respectively CCDC 916549−916553) are provided in the Supporting Information.

■ ASSOCIATED CONTENT

Ⓢ Supporting Information

Figures, tables, and CIF files giving ^{1}H, ^{13}C and ^{31}P NMR spectra for all alkylated phosphole oxides, X-ray crystallographic data of phosphole oxides, and DFT calculation details, including geometries and energies for calculated structures, shielding tensors, and full scan data for the PES calculations. This material is available free of charge via the Internet at http://pubs.acs.org.

■ AUTHOR INFORMATION

Corresponding Author

*E.M.E.V.: tel, +44 (0) 1273 678621; e-mail, e.m.e.viseux@sussex.ac.uk.

Notes

The authors declare no competing financial interest.

■ ACKNOWLEDGMENTS

This work was supported in part by a Bader award. We also thank Dr. John Turner and Dr. Ian Crossley for useful discussions and Dr. Hazel Cox and Mr. Gavin Roffe for support in the theoretical side of our research. We thank Dr. Iain Day for the NMR service and Dr. Ali Abdul Sadaa for mass spectroscopy and useful discussions.

■ REFERENCES

(1) Matano, Y.; Nakashima, M.; Saito, A.; Imahori, H. *Org. Lett.* **2009**, *11*, 3338−3341.
(2) Coe, B. J.; Curati, N. R. M. *Comments Inorg. Chem.* **2004**, *25*, 147−184.
(3) Rubbiani, R.; Kitanovic, I.; Alborzinia, H.; Can, S.; Kitanovic, A.; Onambele, L. A.; Stefanopoulou, M.; Geldmacher, Y.; Sheldrick, W. S.; Wolber, G.; Prokop, A.; Woelfl, S.; Ottt, I. *J. Med. Chem.* **2010**, *53*, 8608−8618.
(4) Bhabak, K. P.; Bhuyan, B. J.; Mugesh, G. *Dalton Trans.* **2011**, *40*, 2099−2111.
(5) Ott, I. *Coordin. Chem. Rev.* **2009**, *253*, 1670−1681.
(6) Matano, Y.; Miyajima, T.; Ochi, N.; Nakabuchi, T.; Shiro, M.; Nakao, Y.; Sakaki, S.; Imahori, H. *J. Am. Chem. Soc.* **2008**, *130*, 990−1002.
(7) Bruijnincx, P.; Sadler, P. J. *Curr. Opin. Chem. Biol.* **2008**, *12*, 197−206.
(8) Shimada, T.; Kurushima, H.; Cho, Y.; Hayashi, T. *J. Org. Chem.* **2001**, *66*, 8854−8858.
(9) Ren, Y.; Baumgartner, T. *Dalton Trans.* **2012**, *41*, 7792−7800.
(10) Wan, J.-H.; Fang, W.-F.; Li, Y.-B.; Xiao, X.-Q.; Zhang, L.-H.; Xu, Z.; Peng, J.-J.; Lai, G.-Q. *Org. Biomol. Chem.* **2012**, *10*, 1459−1466.
(11) Bouit, P.-A.; Escande, A.; Szűcs, R.; Szieberth, D.; Lescop, C.; Nyulászi, L.; Hissler, M.; Réau, R. *J. Am. Chem. Soc.* **2012**, *134*, 6524−6527.
(12) Morisaki, Y.; Aiki, Y.; Chujo, Y. *Macromolecules* **2003**, *36*, 2594−2597.
(13) Bulbrook, M.; Chu, M.; Deane, K.; Doyle, R. J.; Hinc, J.; Peterson, C.; Salem, G.; Thorman, N.; Willis, A. C. *Dalton Trans.* **2010**, *39*, 8878−8881.
(14) Garner, A. Y.; Tedeschi, A. A. *J. Am. Chem. Soc.* **1962**, *84*, 4734−&.
(15) Dogan, J.; Schulte, J.; Swiegers, G.; Wild, S. B. *J. Org. Chem.* **2000**, *65*, 951−957.
(16) Stankevic, M.; Pietrusiewicz, K. M. *Tetrahedron Lett.* **2009**, *50*, 7093−7095.
(17) Cereghetti, M.; Arnold, W.; Broger, E. A.; Rageot, A. *Tetrahedron Lett.* **1996**, *37*, 5347−5350.
(18) Vandoorn, J. A.; Frijns, J.; Meijboom, N. *Recl. Trav. Chim. Pays-Bas* **1991**, *110*, 441−449.
(19) Brooks, P.; Gallagher, M. J.; Sarroff, A. *Aust. J. Chem.* **1987**, *40*, 1341−1351.
(20) Gladiali, S.; Dore, A.; Fabbri, D.; Delucchi, O.; Valle, G. *J. Org. Chem.* **1994**, *59*, 6363−6371.
(21) Dogan, J.; Schulte, J.; Swigers, G.; Wild, S. *J. Org. Chem.* **2000**, *65*, 4782−4782.
(22) Maryasin, B.; Zipse, H. *Phys. Chem. Chem. Phys.* **2011**, *13*, 5150.
(23) Lodewyk, M. W.; Siebert, M. R.; Tantillo, D. J. *Chem. Rev.* **2012**, *112*, 1839−1862.
(24) Sarotti, A. M.; Pellegrinet, S. C. *J. Org. Chem.* **2009**, *74*, 7254−7260.
(25) Britt, A. D.; Kaiser, E. T. *J. Phys. Chem.* **1965**, *69*, 2775−2779.
(26) Tunney, S. E.; Stille, J. K. *J. Org. Chem.* **1987**, *52*, 748−753.
(27) Holz, J.; Monsees, A.; Kadyrov, R.; Börner, A. *Synlett* **2007**, 599−602.
(28) Britt, A. D.; Kaiser, E. T. *J. Org. Chem.* **1966**, *31*, 112−114.
(29) Raghunath, M.; Zhang, X. *Tetrahedron Lett.* **2005**, *46*, 8213−8216.